Title

Gravity-driven transport of three engineered nanomaterials in unsaturated soils and their effects on soil pH and nutrient release

Authors

Conway, Jon R

Keller, Arturo A

Publication Date

2016-07-01

DOI

10.1016/j.watres.2016.04.021

Peer reviewed

Water Research 98 (2016) 250–260

Contents lists available at ScienceDirect

Water Research

journal homepage: www.elsevier.com/locate/watres

Gravity-driven transport of three engineered nanomaterials in unsaturated soils and their effects on soil pH and nutrient release

Jon R. Conway [a, b], Arturo A. Keller [a, b, *]

[a] Bren School of Environmental Science and Management, University of California, Santa Barbara, CA 93106, USA
[b] University of California Center for the Environmental Implications of Nanotechnology (UC CEIN), USA

ARTICLE INFO

Article history:
Received 10 December 2015
Received in revised form
11 April 2016
Accepted 12 April 2016
Available online 13 April 2016

Keywords:
Engineered nanomaterials
TiO_2
CeO_2
$Cu(OH)_2$
Soil transport
Nutrient release

ABSTRACT

The gravity-driven transport of TiO_2, CeO_2, and $Cu(OH)_2$ engineered nanomaterials (ENMs) and their effects on soil pH and nutrient release were measured in three unsaturated soils. ENM transport was found to be highly limited in natural soils collected from farmland and grasslands, with the majority of particles being retained in the upper 0–3 cm of the soil profile, while greater transport depth was seen in a commercial potting soil. Physical straining appeared to be the primary mechanism of retention in natural soils as ENMs immediately formed micron-scale aggregates, which was exacerbated by coating particles with Suwannee River natural organic matter (NOM) which promote steric hindrance. Small changes in soil pH were observed in natural soils contaminated with ENMs that were largely independent of ENM type and concentration, but differed from controls. These changes may have been due to enhanced release of naturally present pH-altering ions (Mg^{2+}, H^+) in the soil *via* substitution processes. These results suggest ENMs introduced into soil will likely be highly retained near the source zone.

1. Introduction

The majority of the production, use, and disposal of engineered nanomaterials (ENMs) occur in the terrestrial environment (Gottschalk and Nowack, 2011; Keller et al., 2013). Due to this, terrestrial ecosystems are and will increasingly be some of the largest receptors of ENMs at all stages of their life cycle. In particular, soil is predicted to be one of the major receptors of ENMs, so in order to effectively regulate ENM use and disposal it is necessary to understand how the interactions between ENMs and soils influence ENM subsurface transport and their effects on soil properties.

ENM mobility in the subsurface is governed by several processes of varying influence, including sorption to organisms and other media components, physical straining through soil pore spaces, and dissolution and pH-induced aggregation. Sorption can occur *via* electrostatic attraction between charged clay surfaces and oppositely-charged ENMs (Zhou et al., 2012) or chemically (for metal oxides or metals with an outer oxide layer) through a dehydration reaction similar to the binding of phosphate or iron oxides to clays (Horst et al., 2010; Hofstetter et al., 2003). Sorption to organic matter (Duester et al., 2011) and organisms (Mudunkotuwa and Grassian, 2010) in soil may take place through similar mechanisms.

There is also the possibility of physical straining, clogging, and collection at air-water-soil interfaces when flowing through porous media (Keller and Auset, 2007; Torkzaban et al., 2015; Cornelis et al., 2013). Physical straining of high aspect ratio ENMs in soil has been demonstrated with single-walled carbon nanotubes (Jaisi and Elimelech, 2009) and implicated as a primary retention mechanism for nanoscale Fe^0 (nZVI) in a sandy loam soil (Basnet et al., 2015). Fang et al. (2016) found that the transport of CeO_2 ENMs through quartz sand and soil was significantly increased with the addition of both continuous and discontinuous macropores, highlighting the importance of straining on ENM movement through porous media. Increasing aggregation caused by high ionic strength, pH near the point of zero charge (PZC), or coatings can result in more physical straining, particularly in soils like Vertisols or Ultisols that are characterized by small pore sizes.

Relatively little research has been done on the effects of ENM exposure on soil properties (for a recent review, see Dror et al.

Abbreviations: CCC, critical coagulation concentration; CEC, cation exchange capacity; DLS, dynamic light scattering; ENM, engineered nanomaterials; ESEM-BSE/EDS, environmental scanning electron microscope with backscattering electron detector and energy-dispersive X-ray spectroscopy; ICP-AES, inductively coupled plasma atomic emission spectrometer; NOM, natural organic matter.

* Corresponding author. Bren School of Environmental Science and Management, University of California, Santa Barbara, CA 93106, USA.
E-mail address: keller@bren.ucsb.edu (A.A. Keller).

http://dx.doi.org/10.1016/j.watres.2016.04.021
0043-1354/

(2015)). ENMs may impact soils by sorbing to clay surfaces (Zhou et al., 2012; Wang et al., 2014) or intercalating into the clay structure (Hilhorst et al., 2014; Cousin et al., 2008), and thus alter soil hydraulic properties (Taha and Taha, 2012). Ben-Moshe et al. (2013) observed that CuO and Fe_3O_4 ENMs did not change the total organic content or macroscopic properties of two types of soil but altered the humic substances in the soils. The authors also observed an effect on the soil microbial community, which has been reported in other studies (*e.g.*, (Ben-Moshe et al., 2013; Cesco et al., 2012; Ge et al., 2011; Collins et al., 2012), but did not attempt to link changes in important soil properties with these effects. VandeVoort et al. (2014) found that silver ENMs could limit denitrification processes in soil, but that the effects were dependent on ENM concentration and coating.

Previous studies in this area suggest that the effects of ENMs on soil properties are somewhat limited, although certain ENMs may impact soil *via* mechanisms not yet considered. For example, metal oxide surfaces are amphoteric, capable of producing both protons (H^+) and hydroxide ions (OH^-), but tend to be predominantly acidic in nature (Boehm, 1971). Due to this, metal oxide ENMs may be able to alter the pH of soil pore water and consequently the overall pH of the soil. If ENMs are able to alter soil pH when present above certain concentrations they may pose a hazard to organisms that rely on the soil for habitat or sustenance. However, soils are typically well-buffered, and may be able to withstand ENM accumulation without changing pH.

Metal oxide ENMs bear many similarities to naturally occurring nano-scale semi-crystalline metal oxide minerals known as short-range order (SRO) minerals. SRO minerals have been shown to influence nutrient availability in natural soils *via* sorptive processes (Grand and Lavkulich, 2015), and metal oxide ENMs may also demonstrate this effect. In particular, metal oxides are well known for their ability to covalently adsorb phosphate ions (PO_4^{3-}) (Boehm, 1971; Daou et al., 2007) and, depending on the strength of this interaction, may prevent organisms from accessing this important nutrient.

In this study, the gravity-driven transport and effects on soil properties of three environmentally relevant ENMs, TiO_2, CeO_2, and $Cu(OH)_2$ (Kocide 3000), were measured in a potting soil, an agricultural soil, and a grassland soil. These particles were selected based on their widespread use and/or life cycle characteristics; for example, TiO_2 ENMs are one of the most common nanomaterials in production (Holden et al., 2014) and are used in a wide variety of industrial and consumer applications that will likely result in their introduction into the terrestrial environment (Weir et al., 2012; Gottschalk et al., 2009; Johnson et al., 2011; Kaegi et al., 2008), such as through the concentration of TiO_2 in biosolids during waste water treatment that are then used as agricultural fertilizer (Gottschalk and Nowack, 2011; Wang et al., 2012). CeO_2 ENMs are used in several common industrial processes and as a catalyst in diesel fuel, where they are expelled in exhaust and deposited from the atmosphere onto the land surface (Park et al., 2008; Batley et al., 2013; Dahle and Arai, 2015). Kocide 3000 is a nano-$Cu(OH)_2$ based pesticide manufactured by DuPont (DuPont, 2010) that is specifically developed to be applied to produce and consequently will be directly or incidentally introduced into soils. In order to determine the influence of transport history, the effects of an organic coating (Suwannee River natural organic matter (NOM)) on ENM transport and impacts on soil properties were also measured.

Four hypotheses were addressed in these series of experiments in order to gain insight into the transport of ENMs under unsaturated conditions, such as are typically found in the topsoils of farmlands or grasslands, as well as their effects on soil pH and nutrient mobility. Our first hypothesis was that ENM transport would be limited to the upper layers of soil, but particles coated with NOM would penetrate further into the soil due to increased electrostatic repulsive forces as a result of their more negative surface charge. Our second hypothesis was that particles would be transported further through potting soil than agricultural or grassland soils due to the greater density and clay contents of the two natural soils causing increased physical straining and electrostatic/chemical sorption. Third, we hypothesized that none of the soils would experience a significant change in pH after spiking with ENMs due to the presence of buffering compounds (such as dolomitic lime) in the soils. Fourth, we hypothesized that these ENMs would bind soil nutrients, including phosphate, and reduce their mobility in the soil.

2. Methods

2.1. Nanomaterial characterization and preparation

Three nanomaterials were used in these experiments: TiO_2, CeO_2, and $Cu(OH)_2$. TiO_2 and CeO_2 nanomaterials used in this experiment are fully characterized in Keller et al. (2010) and $Cu(OH)_2$ is characterized in Adeleye et al. (2014). A summary of relevant properties can be found in Table 1. TiO_2 and CeO_2 ENMs were provided by Evonik Degussa Corp. (U.S.) and Meliorum Technologies (U.S.), respectively. $Cu(OH)_2$ particles were purchased from DuPont as the commercially available agricultural biocide Kocide 3000. TiO_2 particles were semispherical with a primary particle size of 27 ± 4 nm with a crystalline structure of 82% anatase and 18% rutile. Particle size after 30 min of sonication in deionized water (DI) was 194 ± 7 nm CeO_2 particles were primarily rods with dimensions of $67 \pm 8 \times 8 \pm 1$ nm with $\leq$10% as polyhedra of diameter 8 ± 1 nm. Crystal structure was ceria cubic and particle size in DI after sonication for 30 min was 231 ± 16 nm. Kocide 3000 is composed of spherical composites on the order of 50 μm made up of irregular nano-to micro-scale $Cu(OH)_2$ embedded in a carbon-based matrix that rapidly dissolves in water to release polydisperse $Cu(OH)_2$ particles approximately 1500 ± 600 nm in diameter.

ENM stock suspensions were prepared by suspending dry ENM powders in 18.2 MΩ cm Nanopure water (Barnstead) and sonicating for 30 min in a bath sonicator (Branson 2510, Danbury, CT). Stock suspensions were sonicated for 10 min after dilution to the desired concentration and used within 24 h. Suwannee River NOM stock solutions were prepared as described in Zhou and Keller (2010a). Hydrodynamic diameter and ζ-potential of TiO_2, CeO_2, and $Cu(OH)_2$ ENMs with and without NOM were measured *via* dynamic light scattering (DLS, Zetasizer Nano ZS-90, Malvern Instruments) at 20 °C by preparing 10 mg L^{-1} ENM suspensions with and without the addition of 1 mg L^{-1} NOM in Nanopure water and in soil solution extracts (described below) through dilution of a 100 mg L^{-1} stock, probe sonicating for 2 s at 20% amplitude (sufficient to disperse aggregates) with a Misonix Sonicator S-4000 (QSonica LLC, Newtown, CT).

2.2. Soil collection and preparation

Three soils were used in this study: a commercial potting soil, a grassland soil, and a farmland soil. Sunshine® Mix #4 potting soil was purchased from Sun Gro (USA), and was composed of peat moss/perlite/dolomitic limestone. Grassland soil was collected from a flat, well drained grassy area at the Sedgwick Reserve in Santa Ynez, CA (N 34° 40′ 33.9″, W 120° 02′ 07.6″), and farmland soil was collected from a fallow field at an organic farm in Carpinteria, CA (N 34° 23′ 34.5″, W 119° 28′ 46.9″). Soil properties can be found in Table 2. Soils were air dried, sieved through a 2 mm mesh, and stored at 4 °C until use. Samples of sieved soil

Table 1
Physicochemical properties of ENMs used in this study.

Property	TiO_2	CeO_2	$Cu(OH)_2$
Primary particle diameter[a] (nm)	27 ± 4	rods: (67 ± 8) × (8 ± 1) (≤10% polyhedra: 8 ± 1 nm)	100–1000
Hydrodynamic diameter[b] (nm)	194 ± 7	231 ± 16	1532 ± 580
Target metal content (wt. %)[c]	98.3	95.14	26.5 ± 0.9
Other elements present[d]	N.M.	N.M.	C, O, Na, Al, Si, S, Zn
Phase/structure	82% anatase, 18% rutile	Cubic ceria	Orthorhombic $Cu(OH)_2$
Morphology	Semispherical	Rods (≤10% polyhedra)	Spherical/polyhedra
Moisture content (wt%)	1.97	4.01	10.84
BET surface area (m^2/g)	51.5	93.8	15.71 ± 0.16
Isoelectric point	6.2	7.5	<3.0
Zeta potential[b] (mV)	+30.0 ± 2.2	+32.8 ± 1.0	−47.6 ± 4.3
pH[b]	4.52	4.51	5.09

[a] Dry powder measured with SEM/TEM.
[b] Measured at 10 mg L^{-1} in Nanopure water.
[c] TiO_2 and CeO_2 purity measured with thermogravimetric analysis (TGA), $Cu(OH)_2$ purity was determined *via* ICP-AES.
[d] Analysis was done *via* XRD and EDS.

Table 2
Properties of soils used in this study.

Property	Potting soil	Grass soil	Farm soil
pH	5.90 ± 0.03	5.90 ± 0.04	6.86 ± 0.02
Electrical conductivity (μS cm^{-1})	474.3 ± 27.9	18.9 ± 0.6	142.1 ± 5.4
Cation exchange capacity (meq 100 g^{-1})	69.2 ± 1.2	25.8 ± 0.1	8.7 ± 0.1
Loss-on-ignition organic matter (%)	52.83 ± 0.91	3.11 ± 0.07	1.44 ± 0.04
Bulk density (g cm^{-3})	0.086 ± 0.001	0.981 ± 0.017	1.101 ± 0.003
Sand/Silt/Clay (%)	N.A.	54.0/29.0/17.0	66.0/22.0/12.0
Saturation percent (%)	514.5 ± 48.4	43.0 ± 0.7	28.0
Water content of air-dry soil (wt. %)	26.91 ± 2.58	10.54 ± 0.02	6.23 ± 0.04
Exchangeable PO_4–P (μg g^{-1})	325.5 ± 2.1	15.3 ± 0.6	51.3 ± 3.0
Exchangeable NH_4–N (μg g^{-1})	10.3 ± 0.0	1.28 ± 0.04	1.69 ± 0.10
Exchangeable NO_3–N (μg g^{-1})	372.3 ± 9.4	11.5 ± 0.5	51.9 ± 0.7
Exchangeable K (μg g^{-1})	1398 ± 6	206 ± 1	278 ± 1
Total Ce (μg g^{-1})	7.0 ± 0.7	30.3 ± 0.8	66.6 ± 0.4
Total Cu (μg g^{-1})	1.2 ± 0.1	25.4 ± 0.3	30.5 ± 0.4
Total Ti (μg g^{-1})	16 ± 0	1864 ± 10	1726 ± 9

were characterized for pH, texture, saturation percent, soluble salts, cation exchange capacity, conductivity, organic content, and exchangeable NH_4, NO_3, K, and PO_4 by the University of California, Davis Analytical Laboratory (http://anlab.ucdavis.edu/). Total Ce, Cu, and Ti concentrations of each soil were measured after digesting ~0.3 g soil samples in 10 mL 1:3 HNO_3:HCl at 200 °C for 1.5 h in a microwave digestion system (Multiwave Eco, Anton Paar) followed by analysis *via* inductively coupled plasma atomic emission spectroscopy (ICP-AES, iCAP 6300 Thermo Scientific, Waltham, MA). Detection limits for all elements tested were approximately 5 μg L^{-1}. Standard solutions and blanks were measured every 15–20 samples for quality assurance. This technique was sufficient to dissolve the soil and 89.6 ± 0.2%, 95.89 ± 9.7, and 100 ± 0.0% of TiO_2, CeO_2, and $Cu(OH)_2$, respectively.

Soil bulk density was measured following McKenzie et al. (2004) and soil solution extracts were prepared following Rhoades (1982), although no Na_3PO_4 was added in order to avoid influencing ENM physicochemical behavior. Briefly, soils were saturated with Nanopure water and allowed to equilibrate overnight before the extract was collected *via* vacuum filtration. Soil solution extracts were stored at 4 °C until use. The water content of air-dried soil was measured also following Rhoades (1982).

2.3. ENM transport through unsaturated soil

ENM transport through the three soils was tested by packing 2.5 cm diameter × 16.34 cm long cylindrical plastic columns (Ray Leach Cone-tainers; Stuewe and Sons, Tangent, Oregon) with 17.5 ± 0.1 g potting soil, 136 ± 1 g grass soil, or 167 ± 1 g farm soil, which was sufficient to fill the columns within 1 cm of the top. Soils were air dried before use. The soil packing density reflects the porosity of disturbed topsoil rather than highly packed deeper soils. The bulk density of packed potting soil is about 12x lower than the natural soils due to its very high organic content (>10x more than the natural soils used here), which is a result of the high proportion of peat moss in its formulation. This potting soil was chosen for this study as to simulate the organic (O) horizon present as the top layer of some soils (Brady and Weil, 2002). To simulate gravity-driven transport of ENMs in suspension, 50 mL of 100 mg L^{-1} TiO_2, CeO_2, or $Cu(OH)_2$ ENM suspensions with or without the addition of 10 mg L^{-1} NOM were applied to the top of the column at a rate of 10 mL min^{-1} and allowed to flow through the column *via* gravity. The resulting soil ENM concentrations were on the high end of those currently predicted for metal oxides in soil (Gottschalk et al., 2013), but were well within the concentrations predicted for biosolids (Gottschalk et al., 2013; Lazareva and Keller, 2014). Hence, the soil ENM concentrations used in this experiment may be indicative of those found in soils repeatedly amended with biosolids.

After ENM application, columns were air dried overnight then oven dried at 60 °C for 72 h. The dried soil was carefully removed from the column in 3 cm segments, ~0.3 g subsamples of which were weighed, and digested in 10 mL 1:3 HNO_3:HCl at 200 °C for 1.5 h in a microwave digestion system (Multiwave Eco, Anton Paar) followed by analysis *via* inductively coupled plasma atomic emission spectroscopy (ICP-AES, iCAP 6300 Thermo Scientific, Waltham, MA). This technique was sufficient to dissolve the soil and ≥90% of TiO_2, CeO_2, and $Cu(OH)_2$. Five replicate columns were prepared and

analyzed for each treatment.

Metal concentrations for all three ENMs are reported as ionic, although neither CeO_2 nor TiO_2 were expected to dissolve to a significant degree under the conditions used in this experiment. TiO_2 is known to be highly insoluble in water and CeO_2 is similarly insoluble at pH similar to those found in the soils used here (Collin et al., 2014). However, $Cu(OH)_2$ has been shown to undergo partial dissolution under acidic to neutral conditions, although at acidic pH less dissolution occurs in media with high concentrations of dissolved organic matter (Adeleye et al., 2014; Conway et al., 2015). Based on this, dissolution of $Cu(OH)_2$ is not expected to occur to a significant degree under the conditions and time scales used in this experiment.

To measure size distribution of particles throughout the column, air-dried samples of contaminated soils were collected from the top and bottom 3 cm of columns and analyzed using environmental scanning electron microscopy (ESEM) with backscattering electron detection (BSE) and energy-dispersive X-ray spectroscopy (EDS) to confirm identification of CeO_2, $Cu(OH)_2$, or TiO_2 ENMs. Beam voltage was set at 12 kV, spot size at 6.0, water vapor pressure was kept at 2.7 Torr, and working distance averaged around 10.5 cm. These settings were chosen in order to minimize X-ray subsurface penetration for EDS analysis. Elemental hypermap data were collected over a period of 6 min per image. ImageJ image analysis software (National Institute of Health, Bethesda, Maryland, USA; available at http://rsbweb.nih.gov/ij) was used to determine particle or aggregate size. Soils not contaminated with ENMs were also tested and used as references. Naturally occurring Ti- and Ce-containing particles were found in reference samples and were identified by the presence of elements not found in the ENMs used, S and Ca in particular.

2.4. ENM impacts on soil properties

The effect of ENM contamination on soil pH was tested over a range of ENM concentrations by spiking 3.00 g samples of potting, grass, or farm soil with either 0, 0.3, or 3 mL of 10 mg L^{-1} TiO_2, CeO_2, or $Cu(OH)_2$ ENM stock suspensions or 0.3 or 3 mL of 100 mg L^{-1} stock to produce ENM concentrations in the soil of 0, 0.1, 1, 10, and 100 μg g^{-1}. ENM stock solutions were prepared with and without the addition of 10 mg L^{-1} NOM and sonicated for 30 min. Soil aliquots were then air dried and vigorously mixed with Nanopure water for 1 min in a 1:5 soil:water ratio to make a soil slurry from which the pH was measured. A 1:5 soil:water ratio was used due to the high absorptive capacity of the potting soil. Samples were mixed continuously for at least 5 min or until the pH had stabilized before a measurement was recorded. All treatments were performed in triplicate.

Changes in soil ion release due to the presence of ENMs was tested by spiking 3.00 g aliquots of potting, grassland, or farm soil with 3 mL of 100 mg L^{-1} TiO_2, CeO_2, or $Cu(OH)_2$ ENM stock suspensions that had been sonicated for 30 min to produce a final soil ENM concentration of 100 μg g^{-1}. Nanopure water was then vigorously mixed into each soil sample for 1 min to produce a 1:5 soil:water slurry, which was centrifuged at 8000 × *g* for 10 min. The supernatant of each sample was collected and analyzed for Al, Ca, Fe, K, Mg, Na, NO_3, P, and S. NO_3^- was measured *via* colorimetric methods (Hach) and Al, Ca, Fe, K, Mg, Na, P, and S were measured *via* ICP-AES after acidification to 10% HNO_3.

The influence of the three ENMs on the bioavailability and mobility of P was investigated further by contaminating 3.00 g samples of agricultural, grassland, or potting soil samples with 3 mL of 100 mg L^{-1} TiO_2, CeO_2, or $Cu(OH)_2$ ENM stock suspensions that had been sonicated for 30 min to produce a final soil ENM concentration of 100 μg g^{-1} and then testing P content in three fractions: water extractable P, bioavailable P, and immobile (soil bound) P. Bray extract (Bray and Kurtz, 1945) was used as a proxy to estimate bioavailable P. Contaminated soil samples were first mixed vigorously with Nanopure water for 1 min to produce a 1:5 soil:water slurry, centrifuged at 8000 × *g* for 10 min, then the supernatant was removed and acidified to 10% HNO_3. The same soil samples were air dried then mixed vigorously with Bray extract for 1 min to produce a 1:5 soil:Bray extract slurry, centrifuged at 8000 × *g* for 10 min, then the supernatant was removed and acidified to 10% HNO_3. The soil samples were again air dried then acid digested in 10 mL of 1:3 HNO_3:HCl at 200 °C for 1.5 h in a microwave digestion system, and all samples were analyzed for P content *via* ICP-AES.

2.5. Statistical analyses

To determine the influence of the presence of NOM coatings, ENM type, and soil solution extract type on ENM hydrodynamic diameter and ζ-potential 3-way ANOVA with interactions and post-hoc Tukey's tests were used. To determine the effects of NOM coatings and ENM concentration on soil pH, 2-way ANOVA with interactions and post-hoc Tukey's tests were used for each ENM and soil type. For the effect of ENM contamination on the release of ions from each soil type, separate Dunnett's tests were used for each ion type using Nanopure-only groups as controls. Levene's test was used to ensure homogeneity of variance. Statistical analyses were performed using Microsoft Excel 2007 and the statistical software R (v. 2.11.1).

3. Results & discussion

3.1. ENM transport through unsaturated soils

Gravity-driven vertical transport of ENMs through unsaturated soil was found in general to follow the hypothesis that the majority of ENMs would be retained in the upper portion of the column, but as predicted was found to be highly dependent on soil type with increased retention occurring in the denser, less porous natural soils (Fig. 1). However, ENMs coated with natural organic matter (NOM) did not have increased vertical transport, and in fact were retained more in potting soil. TiO_2 and CeO_2 aggregate sizes (Fig. 2) were seen to decrease with column depth, suggesting physical straining to be the primary impediment to transport. Aggregate hydrodynamic diameters tended to be larger in soil solution extracts than in Nanopure H_2O and were also generally larger than NOM-coated particles, with several exceptions (Fig. 3). Since the soils were unsaturated and the flow rate did not fully saturate the soils, breakthrough of the suspension water was observed at the bottom of the columns, likely through the movement of thin water films (Keller and Sirivithayapakorn, 2004). In potting soil breakthrough occurred during ENM application or within 5 min, while in grassland and agricultural soils it occurred within 1–2 h due to their greater density.

All three ENMs in general passed through the entire length of potting soil columns, being present in lower concentrations than the hypothetical homogeneous concentrations at all points, although there was some retention in the upper 0–6 cm that was increased with NOM-coated particles (Fig. 1A–C). The remainder of the ENMs added to the columns drained out through the bottom of the column. These trends can likely be explained by the primarily organic composition of the potting soil, which gave it very low density, high porosity, and high reactivity (as shown by the high CEC in Table 2). The low density and high porosity prevented aggregates from being physically strained, which is shown for TiO_2 and CeO_2 by the similar aggregate sizes in the tops and bottoms of

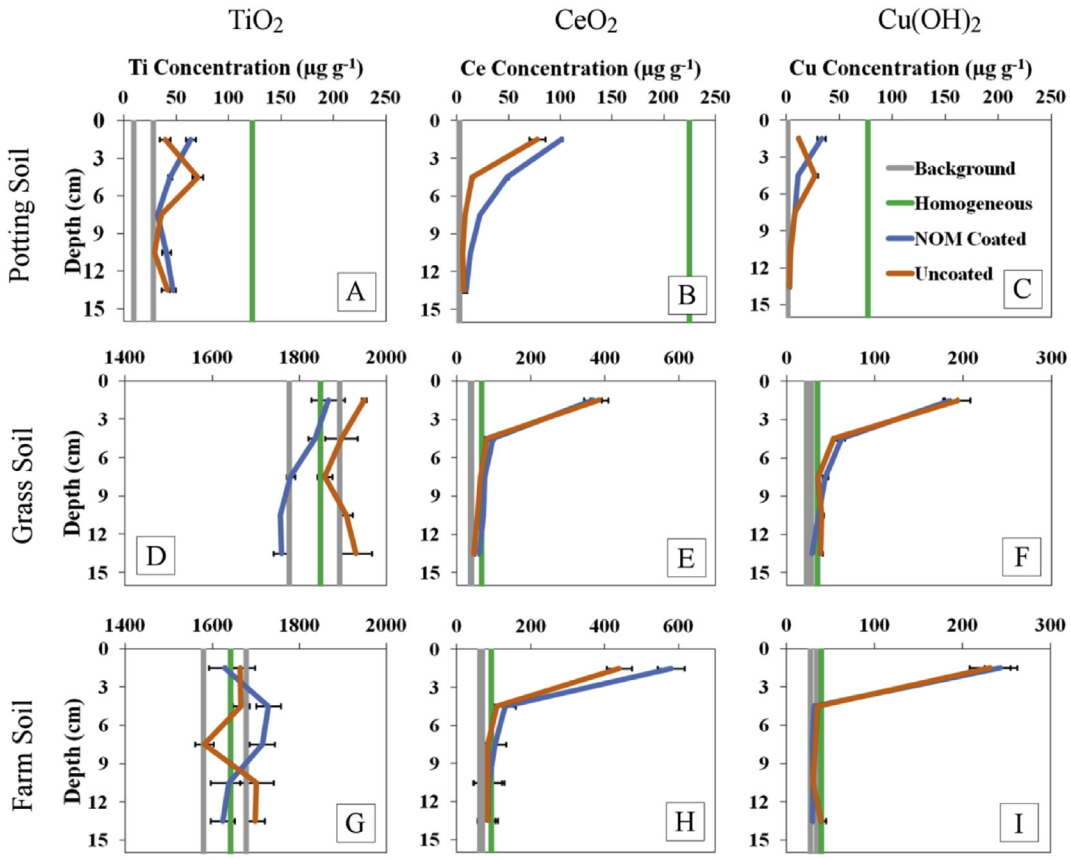

Fig. 1. Gravity-driven transport of suspended uncoated and NOM-coated TiO_2, CeO_2, and $Cu(OH)_2$ ENMs through potting, grass, and farm soil columns. Each point represents the average concentration of a 3 cm vertical segment of a column (*i.e.*, 0–3 cm, 3–6 cm, etc.). For reference, grey lines show the range of background concentrations of target metals present naturally in soils (mean ± 1 SD) and green lines represent hypothetical concentrations that would be found if the ENMs were mixed homogeneously throughout the entire column. Error bars are ±1 SE. Note variable x-axis. (For interpretation of the references to colour in this figure legend, the reader is referred to the web version of this article.)

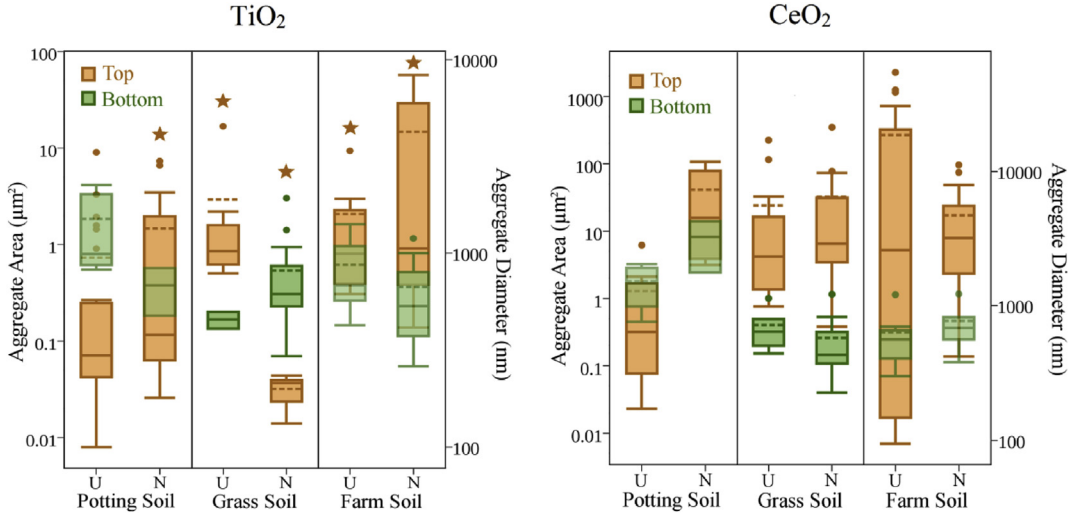

Fig. 2. Tukey box plots of aggregate size distributions of uncoated (U) or NOM-coated (N) TiO_2 and CeO_2 ENMs in potting soil, grass soil, and farm soil measured by electron micrograph analysis. Aggregate areas (in μm^2) were estimated from micrographs and aggregate diameter (in nm) was calculated by considering aggregates as spheres in order to provide comparison to Fig. 3. Samples taken from the upper 0–3 cm of the column are shown in orange (Top) and samples taken from the lower 12–15 cm of the column are shown in green (Bottom). Means are represented as dashed lines and outliers are shown as dots. Stars indicate samples in which large continuous surface deposits of TiO_2 were seen, which are not included in the aggregate size distributions shown here. $Cu(OH)_2$ aggregates could not be positively identified with BSE/EDS due to the low Cu content of the $Cu(OH)_2$ particles as well as the relatively low atomic mass of Cu. Note variable y-axis. (For interpretation of the references to colour in this figure legend, the reader is referred to the web version of this article.)

columns for both uncoated and NOM-coated particles (Fig. 2). If physical straining was strongly influencing particle transport in

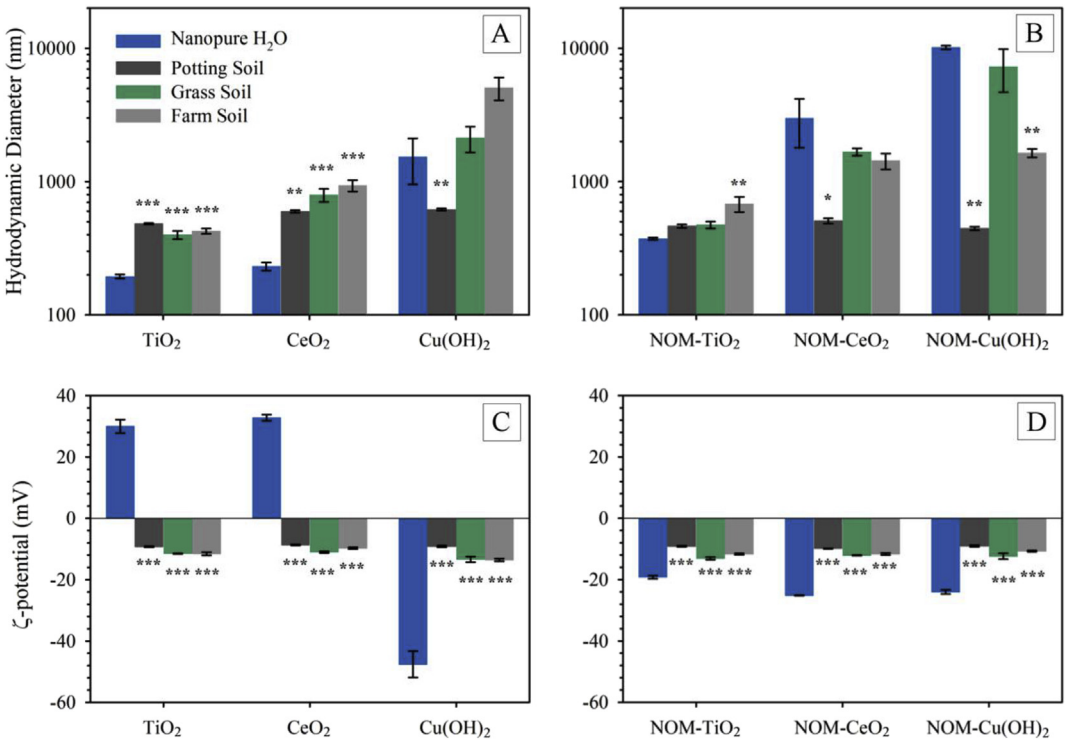

Fig. 3. Hydrodynamic diameter (A & B) and ζ-potential (C & D) of TiO_2, CeO_2, and $Cu(OH)_2$ ENMs at a concentration of 10 mg L^{-1} with and without 1 mg L^{-1} NOM in Nanopure water or soil solution extracts from potting, grass, and farm soil. Asterisks represent significance differences between ENMs in soil solution extracts to ENMs in Nanopure water from ANOVA with post-hoc Tukey's tests. $^{*}p < 0.05$, $^{**}p < 0.01$, $^{***}p < 0.005$. Error bars are ± SE.

potting soil it is unlikely similar aggregate sizes would be observed throughout the length of the column, but rather would result in smaller aggregates or particles penetrating through the column while larger aggregates would be retained at the surface – as was seen in the two natural soils. All three ENMs had similar hydrodynamic diameters in potting soil solution (Fig. 3A–B), although NOM-coated aggregates were significantly smaller than uncoated aggregates (3-way ANOVA, $p < 0.0001$). ζ-potentials for all three ENMs in soil solutions from all three soils were also similar (Fig. 3C–D), although again the presence of NOM coatings, as well as the ENM and soil types, influenced the ζ-potentials (3-way ANOVA, $p < 0.05$).

Coating particles with NOM appears to increase their affinity for the organic components of the potting soil, possibly via entanglement (i.e. steric hindrance). This resulted in the increased overall retention of NOM-coated CeO_2 (Fig. 1B) as well as the decreased vertical transport of NOM-coated TiO_2 and $Cu(OH)_2$ (Fig. 1A and C). Evidence for this can be found in Fig. 3A–B, which show that both NOM-coated and uncoated aggregates have nearly identical hydrodynamic diameters in potting soil solution extract, so the additional retention of NOM-coated aggregates is unlikely to be due to increased physical straining. This was visually confirmed in micrographs of NOM-coated TiO_2 in potting soil including Fig. 4D, which revealed the formation of TiO_2 deposits occurring primarily on the organic peat moss of the potting soil over the Al/Si/Na/K perlite minerals. These deposits may have been caused in part due to interactions between the NOM coating and the organic matter in the potting soil. This finding is counter to several previous transport studies using TiO_2 (Ben-Moshe et al., 2010), CeO_2 (Lv et al., 2014), and ZnO (Kurlanda-Witek et al., 2014) in quartz sand that found organic coatings decreased ENM retention by increasing electrostatic repulsion between coated aggregates and the sand grains, which further suggests interactions between the organic coating and organic soil components.

In the grassland and agricultural soils CeO_2 and $Cu(OH)_2$ shared similar transport profiles (Fig. 1), forming large aggregates in the soil solutions (Fig. 3) that were retained almost entirely in the upper 0–3 cm of the soil columns. However, the widely variable background concentrations of Ti in these natural soils prevented precise measurement of TiO_2 ENM distribution throughout the soil columns by ICP-AES (Fig. 1D and G). The majority of TiO_2 aggregates were confirmed to be retained immediately at the surface through both visual identification of white buildup on the column surfaces and through BSE/EDS analysis. As shown in Fig. 4, both uncoated and NOM-coated TiO_2 ENMs formed large deposits on the surfaces of all three soils with the exception of uncoated TiO_2 in potting soil.

CeO_2 ENMs followed clear trends of transport across soil type, forming large porous aggregates (Fig. 5) that were retained primarily at the surface (Fig. 1). Similar to the trends seen with TiO_2, CeO_2 aggregate size decreased with increasing column depth as larger aggregates were strained by the soil matrix (Fig. 2). However, despite having nearly identical surface charges in soil solution extracts (Fig. 3A), CeO_2 formed large porous sponge-like aggregates instead of the more solid deposits seen with TiO_2. These differences in aggregate morphology may be due to differences between the primary particle shapes of these two ENMs, with TiO_2 being nanospheres and CeO_2 being nanorods. Afrooz et al. (2013) found that spherical Au ENMs had higher attachment efficiencies and deposition rates than rod-like Au ENMs identical in composition, which they attributed to differences in electrosteric and physical packing characteristics. Similarly, Zhou et al. (2013) found the critical coagulation concentration (CCC) of TiO_2 nanospheres was directly related to particle diameter while the CCC of TiO_2 nanorods was better explained by particle surface area, which they postulated was a consequence of differences in exposed crystal faces. It has also been shown that metal oxide nanospheres and nanorods

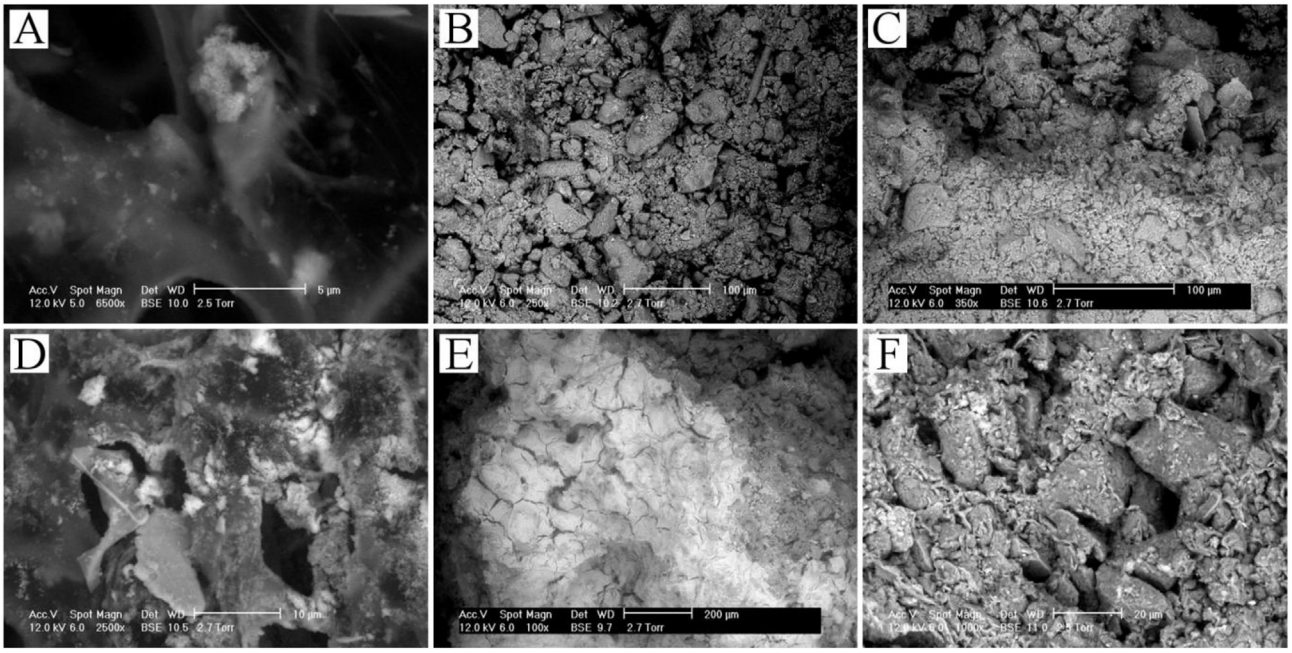

Fig. 4. Surface deposits (lighter areas) of uncoated (top row) and NOM-coated (bottom row) TiO_2 in potting soil (A & D), grass soil (B & E), and farm soil (C & F). Micrographs were taken of partially hydrated samples (2.7 torr) from the upper 0–3 cm of columns using ESEM with BSE. Large continuous deposits were not found with uncoated TiO_2 in potting soil (A) or grass soil (B). Scale varies between images. EDS element maps of Ti for these images can be found in Figure S1.

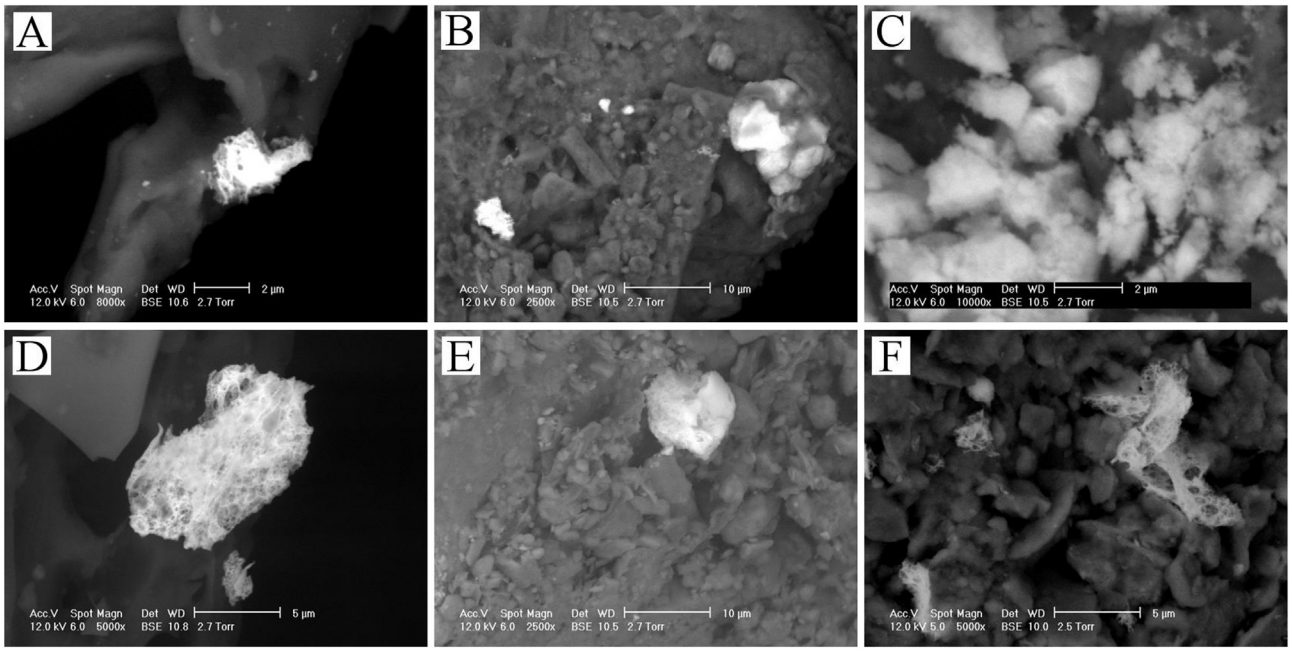

Fig. 5. Aggregates of uncoated (top row) and NOM-coated (bottom row) CeO_2 in potting soil (A & D), grass soil (B & E), and farm soil (C & F). Micrographs were taken of partially hydrated samples (2.7 torr) from the upper 0–3 cm of columns using ESEM with BSE. Scale varies between images. EDS element maps of Ce for these images can be found in Figure S2.

interact differently with NOM (Zhou et al., 2013; Zhou and Keller, 2010b), which may also be a factor in explaining the differences in aggregate morphology seen here.

Although no $Cu(OH)_2$ aggregates or particles could be identified by ESEM-BSE/EDS due to the low atomic weight of Cu and low Cu content of the $Cu(OH)_2$ particles, it is likely that physical straining was also the primary mechanism of retention since $Cu(OH)_2$ particles displayed similar transport profiles to CeO_2. This hypothesis is supported by Fig. 3, which shows that $Cu(OH)_2$ aggregate sizes in soil solutions are equal to or larger than TiO_2 or CeO_2. Despite the low to moderate solubility of $Cu(OH)_2$ particles (10–20% over 24 h at circumneutral pH) (Adeleye et al., 2014; Conway et al., 2015), it is not likely significant dissolution occurred in these transport experiments given that both uncoated and NOM-coated $Cu(OH)_2$ had nearly identical transport profiles to the relatively insoluble CeO_2 (Dahle and Arai, 2015).

These results suggest that these and other ENMs similar in size and/or aggregation tendencies will primarily be retained in the immediate area of contamination and may potentially accumulate to high concentrations that may adversely affect local organisms. Additionally, since these ENMs appear to be able to pass relatively unimpeded through potting soil, which approximates the organic (O) horizon present in some soils, there may be accumulation of ENMs at the boundary between the O horizon and the underlying mineral horizon.

3.2. ENM effects on soil properties

Despite varying ENM concentrations over four orders of magnitude, changes in soil pH due to ENM contamination were largely independent of both ENM type and concentration (Fig. 6). Contrary to the first hypothesis, changes in soil pH due to ENM contamination did occur, but they were found to be highly dependent on soil type. All three ENMs increased grass soil pH (2-way ANOVA, $p < 0.05$, Fig. 6C), decreased farm soil pH when uncoated (2-way ANOVA, $p < 0.05$, Fig. 6E), and, with the exception of NOM-coated $Cu(OH)_2$ (2-way ANOVA, $p < 0.05$), had no effect on potting soil pH (2-way ANOVA, $p > 0.05$, Fig. 6A). Additionally, the presence of NOM had no effect on the influence of ENMs on soil pH except in the case of farm soil, where a slight buffering effect was seen for CeO_2 and $Cu(OH)_2$ (2-way ANOVA, $p < 0.05$, Fig. 6F). As nearly all changes in soil pH due to ENM contamination were independent of ENM concentration it is unlikely these ENMs directly influenced soil pH through the production of H^+/OH^- as a result of their amphoteric properties. One possible alternate explanation is that the ENMs increased the release of ions that act as buffering or pH-altering agents, such as Al^{3+}, Ca^{2+}, H^+, K^+, Mg^{2+}, Na^+, and OH^-, by replacing them on the mineral surfaces of the soil matrix. Since there is a limited pool of ions available for desorption in a unit of soil, changes in ion release due to ENM sorption would be relatively independent of ENM concentration beyond the point at which total sorption/desorption occurs.

Evidence for this can be found in Fig. 7, which reveals that, contrary to the second hypothesis, these ENMs in fact increase ion release from contaminated soils. However, the identity and amounts of ions released was dependent on soil type, with the total change in ion release for a given soil being roughly proportional to its CEC (Table 2). Fig. 7B shows that all three ENMs increase release of Mg^{2+} in grass soil, which may be the cause of the pH increases seen in grass soil (Fig. 6C) since Mg^{2+} is a basic cation. While no consistent corresponding changes in ion concentration were seen in farm soil, the decreases in pH may have been due to the release of H^+ stored in the soil. The farm soil used here had relatively low amounts of basic Mg^{2+} and K^+ and low cation exchange capacity (8.7 ± 0.1 meq 100 g^{-1}) and so had the lowest buffering capacity of the soils in this study. Potting soil had the highest concentrations of basic ions and CEC (69.2 ± 1.2 meq 100 g^{-1}) and correspondingly showed no changes in pH due to the presence of ENMs. $Cu(OH)_2$

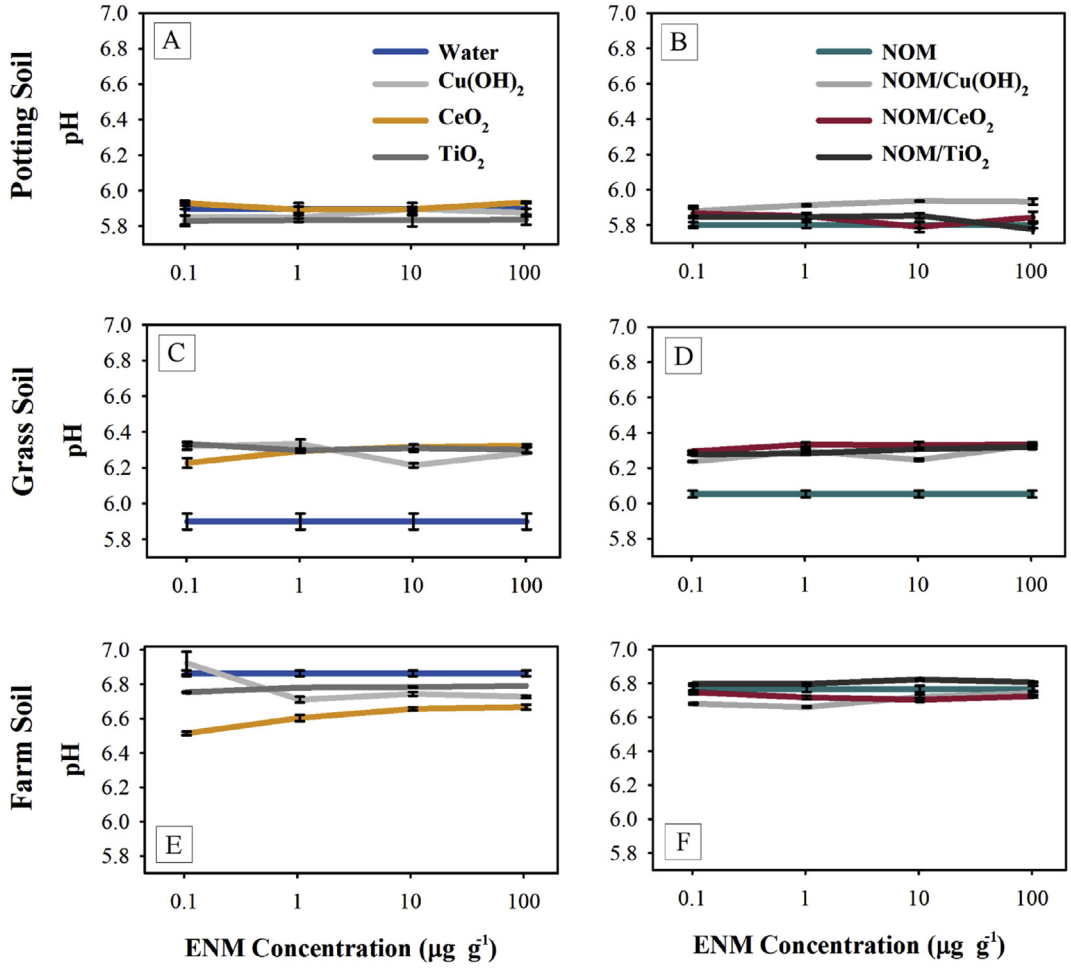

Fig. 6. Changes in pH of potting, grass, and farm soil spiked with increasing concentrations of uncoated (A, C, E) and NOM-coated (B, D, F) TiO_2, CeO_2, and $Cu(OH)_2$ ENMs. Error bars are ± SE.

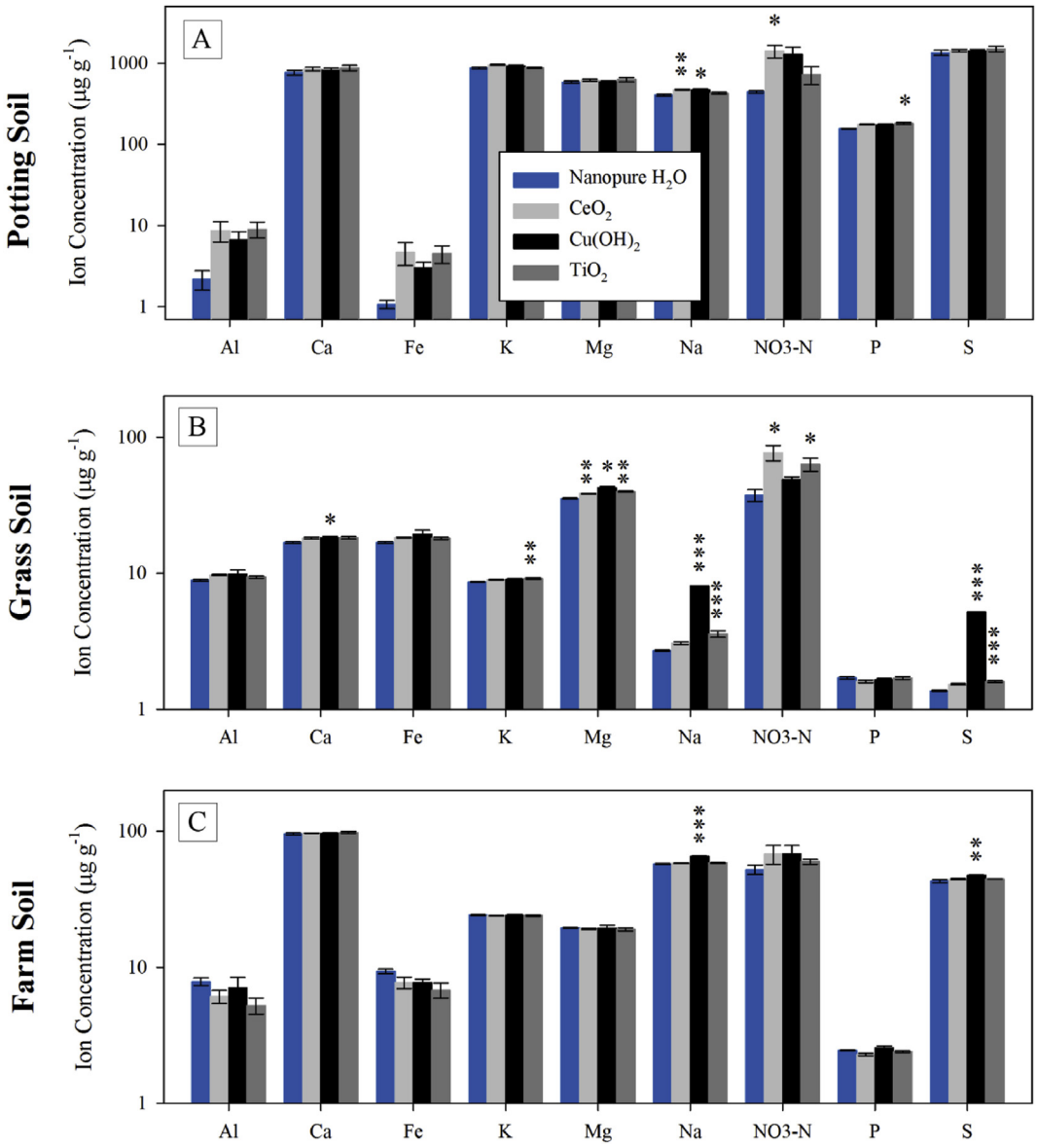

Fig. 7. Changes in ion content of soil solutions extracted from potting, grass, and farm soil after contamination with 100 µg g^{-1} CeO_2, $Cu(OH)_2$, and TiO_2 ENMs. Asterisks represent significance differences between ion concentrations from contaminated and control soil solution extracts from Dunnett's tests. $^{*}p < 0.05$, $^{**}p < 0.01$, $^{***}p < 0.005$. Error bars are ± SE. Note variable y-axis.

consistently increased soil Na and S levels because both of these elements are major components of the soluble composite matrix the $Cu(OH)_2$ ENMs are embedded in and are released as the composite dissolves in water. Similarly, it was found that these ENMs either had no effect or slightly increased the amount of water extractable or bioavailable P (Figure S3). Additionally, since these ENMs already possess or rapidly develop negative surface charges in soil solution (Fig. 3C) they are unlikely to attract negatively charged phosphate ions as readily and thus would not inhibit their mobility or bioavailability.

4. Conclusions

The results of this study suggest that localized hotspots of highly contaminated soil may be more common than large areas of more diffuse concentrations. Our results indicate that, at least in the short term, the majority of the ENMs would be retained in the first few centimeters, with reduced transport to deeper soils. However, there is a potential for deeper transport with repeated application of biosolids and irrigation or rainfall, which needs to be studied in longer-term experiments. These results also justify for some scenarios the use of higher ENM concentrations in toxicity tests for soil organisms than those currently predicted from generalized release estimates. Additionally, we found that ENM contamination at parts per billion concentrations could influence soil pH by enhancing ion release from the soil, although the effect was relatively minor and highly dependent on soil properties. In addition to the implications for soil pH, enhancing the release of ions may have the effect of improving accessibility to these nutrients by organisms in the short term but may also increase the rate at which they are washed from the soil by rainfall or irrigation, resulting in increased nutrient loss and decreased productivity over time.

Author contributions

The manuscript was written through contributions of all authors. All authors have given approval to the final version of the manuscript.

Acknowledgment

This work was supported in part by the National Science Foundation and the U.S. Environmental Protection Agency under Cooperative Agreement #NSF-EF0830117, and by National Science Foundation Grant EF-0742521. Any opinions, findings, and conclusions or recommendations expressed in this material are those of the authors and do not necessarily reflect the views of the National Science Foundation or the U.S. Environmental Protection Agency. The authors would like to thank Arielle Beaulieu, Nicole Beaulieu, Amy Stuyvesant, Lillian Burns, and Ashley Noriega for their assistance with this study. The MRL Shared Experimental Facilities are supported by the MRSEC Program of the NSF under Award No. DMR 1121053; a member of the NSF-funded Materials Research Facilities Network.

Appendix A. Supplementary data

Supplementary data related to this article can be found at http://dx.doi.org/10.1016/j.watres.2016.04.021.

References

Adeleye, A.S., Conway, J.R., Perez, T., Rutten, P., Keller, A.A., 2014. Influence of extracellular polymeric substances on the long-term fate, dissolution, and speciation of copper-based nanoparticles. Environ. Sci. Technol. 48 (21), 12561–12568.

Afrooz, A., Sivalapalan, S.T., Murphy, C.J., Hussain, S.M., Schlager, J.J., Saleh, N.B., 2013. Spheres vs. rods: the shape of gold nanoparticles influences aggregation and deposition behavior. Chemosphere 91 (1), 93–98.

Basnet, M., Di Tommaso, C., Ghoshal, S., Tufenkji, N., 2015. Reduced transport potential of a palladium-doped zero valent iron nanoparticle in a water saturated loamy sand. Water Res. 68, 354–363.

Batley, G.E., Halliburton, B., Kirby, J.K., Doolette, C.L., Navarro, D., McLaughlin, M.J., Veitch, C., 2013. Characterization and ecological risk assessment of nanoparticulate CeO2 as a diesel fuel catalyst. Environ. Toxicol. Chem. 32 (8), 1896–1905.

Ben-Moshe, T., Dror, I., Berkowitz, B., 2010. Transport of metal oxide nanoparticles in saturated porous media. Chemosphere 81 (3), 387–393.

Ben-Moshe, T., Frenk, S., Dror, I., Minz, D., Berkowitz, B., 2013. Effects of metal oxide nanoparticles on soil properties. Chemosphere 90 (2), 640–646.

Boehm, H.P., 1971. Acidic and basic properties of hydroxylated metal oxide surfaces. Discuss. Faraday Soc. 52 (0), 264–275.

Brady, N.C., Weil, R.R., 2002. Elements of the Nature and Properties of Soils. Pearson Education Ltd., Upper Saddle River, New Jersey.

Bray, R.H., Kurtz, L.T., 1945. Determination of total, organic, and available forms of phosphorous in soils. Soil Sci. 59 (1), 39–45.

Cesco, S., Mimmo, T., Tonon, G., Tomasi, N., Pinton, R., Terzano, R., Neumann, G., Weisskopf, L., Renella, G., Landi, L., Nannipieri, P., 2012. Plant-borne flavonoids released into the rhizosphere: impact on soil bio-activities related to plant nutrition. A review. Biol. Fertil. Soils 48 (2), 123–149.

Collin, B., Auffan, M., Johnson, A.C., Kaur, I., Keller, A.A., Lazareva, A., Lead, J.R., Ma, X.M., Merrifield, R.C., Svendsen, C., White, J.C., Unrine, J.M., 2014. Environmental release, fate and ecotoxicological effects of manufactured ceria nanomaterials. Environ. Sci. Nano 1 (6), 533–548.

Collins, D., Luxton, T., Kumar, N., Shah, S., Walker, V.K., Shah, V., 2012. Assessing the impact of copper and zinc oxide nanoparticles on soil: a field study. PLoS One 7 (8).

Conway, J.R., Adeleye, A.S., Gardea-Torresdey, J., Keller, A.A., 2015. Aggregation, dissolution, and transformation of copper nanoparticles in natural waters. Environ. Sci. Technol. 49 (5), 2749–2756.

Cornelis, G., Pang, L.P., Doolette, C., Kirby, J.K., McLaughlin, M.J., 2013. Transport of silver nanoparticles in saturated columns of natural soils. Sci. Total Environ. 463, 120–130.

Cousin, F., Cabuil, V., Grillo, I., Levitz, P., 2008. Competition between entropy and electrostatic interactions in a binary colloidal mixture of spheres and platelets. Langmuir 24 (20), 11422–11430.

Dahle, J.T., Arai, Y., 2015. Environmental geochemistry of cerium: applications and toxicology of cerium oxide nanoparticles. Int. J. Environ. Res. Public Health 12 (2), 1253–1278.

Daou, T.J., Begin-Colin, S., Grenèche, J.M., Thomas, F., Derory, A., Bernhardt, P., Legaré, P., Pourroy, G., 2007. Phosphate adsorption properties of magnetite-based nanoparticles. Chem. Mater. 19 (18), 4494–4505.

Dror, I., Yaron, B., Berkowitz, B., 2015. Abiotic soil changes induced by engineered nanomaterials: a critical review. J. Contam. Hydrol. 181, 3–16.

Duester, L., Prasse, C., Vogel, J.V., Vink, J.P.M., Schaumann, G.E., 2011. Translocation of Sb and Ti in an undisturbed floodplain soil after application of Sb2O3 and TiO2 nanoparticles to the surface. J. Environ. Monit. 13 (5), 1204–1211.

DuPont, 2010. Material Safety Data Sheet: DuPont Kocide 3000 Fungicide/Bactericide.

Fang, J., Wang, M.H., Lin, D.H., Shen, B., 2016. Enhanced transport of CeO2 nanoparticles in porous media by macropores. Sci. Total Environ. 543, 223–229.

Ge, Y.G., Schimel, J.P., Holden, P.A., 2011. Evidence for negative EFFECTS of TiO2 and Zno nanoparticles on soil bacterial communities. Environ. Sci. Technol. 45 (4), 1659–1664.

Gottschalk, F., Nowack, B., 2011. The release of engineered nanomaterials to the environment. J. Environ. Monit. 13 (5), 1145–1155.

Gottschalk, F., Sonderer, T., Scholz, R.W., Nowack, B., 2009. Modeled environmental concentrations of engineered nanomaterials (TiO2, ZnO, Ag, CNT, fullerenes) for different regions. Environ. Sci. Technol. 43 (24), 9216–9222.

Gottschalk, F., Sun, T.Y., Nowack, B., 2013. Environmental concentrations of engineered nanomaterials: review of modeling and analytical studies. Environ. Pollut. 181, 287–300.

Grand, S., Lavkulich, L.M., 2015. Short-range order mineral phases control the distribution of important macronutrients in coarse-textured forest soils of coastal British Columbia, Canada. Plant Soil 390 (1–2), 77–93.

Hilhorst, J., Meester, V., Groeneveld, E., Dhont, J.K.G., Lekkerkerker, H.N.W., 2014. Structure and rheology of mixed suspensions of montmorillonite and silica nanoparticles. J. Phys. Chem. B 118 (40), 11816–11825.

Hofstetter, T.B., Schwarzenbach, R.P., Haderlein, S.B., 2003. Reactivity of Fe(II) species associated with clay minerals. Environ. Sci. Technol. 37 (3), 519–528.

Holden, P.A., Klaessig, F., Turco, R.F., Priester, J.H., Rico, C.M., Avila-Arias, H., Mortimer, M., Pacpaco, K., Gardea-Torresdey, J.L., 2014. Evaluation of exposure concentrations used in assessing manufactured nanomaterial environmental hazards: are they relevant? Environ. Sci. Technol. 48 (18), 10541–10551.

Horst, A.M., Neal, A.C., Mielke, R.E., Sislian, P.R., Suh, W.H., Maedler, L., Stucky, G.D., Holden, P.A., 2010. Dispersion of TiO2 nanoparticle agglomerates by Pseudomonas aeruginosa. Appl. Environ. Microbiol. 76 (21), 7292–7298.

Jaisi, D.P., Elimelech, M., 2009. Single-walled carbon nanotubes exhibit limited transport in soil columns. Environ. Sci. Technol. 43 (24), 9161–9166.

Johnson, A.C., Bowes, M.J., Crossley, A., Jarvie, H.P., Jurkschat, K., Jurgens, M.D., Lawlor, A.J., Park, B., Rowland, P., Spurgeon, D., Svendsen, C., Thompson, I.P., Barnes, R.J., Williams, R.J., Xu, N., 2011. An assessment of the fate, behaviour and environmental risk associated with sunscreen TiO2 nanoparticles in UK field scenarios. Sci. Total Environ. 409 (13), 2503–2510.

Kaegi, R., Ulrich, A., Sinnet, B., Vonbank, R., Wichser, A., Zuleeg, S., Simmler, H., Brunner, S., Vonmont, H., Burkhardt, M., Boller, M., 2008. Synthetic TiO(2) nanoparticle emission from exterior facades into the aquatic environment. Environ. Pollut. 156 (2), 233–239.

Keller, A.A., Auset, M., 2007. A review of visualization techniques of biocolloid transport processes at the pore scale under saturated and unsaturated conditions. Adv. Water Resour. 30 (6–7), 1392–1407.

Keller, A.A., Sirivithayapakorn, S., 2004. Transport of colloids in unsaturated porous media: explaining large-scale behavior based on pore-scale mechanisms. Water Resour. Res. 40 (12), 8.

Keller, A.A., Wang, H.T., Zhou, D.X., Lenihan, H.S., Cherr, G., Cardinale, B.J., Miller, R., Ji, Z.X., 2010. Stability and aggregation of metal oxide nanoparticles in natural aqueous matrices. Environ. Sci. Technol. 44 (6), 1962–1967.

Keller, A.A., McFerran, S., Lazareva, A., Suh, S., 2013. Global life cycle releases of engineered nanomaterials. J. Nanoparticle Res. 15 (6).

Kurlanda-Witek, H., Ngwenya, B.T., Butler, I.B., 2014. Transport of bare and capped zinc oxide nanoparticles is dependent on porous medium composition. J. Contam. Hydrol. 162, 17–26.

Lazareva, A., Keller, A.A., 2014. Estimating potential life cycle releases of engineered nanomaterials from wastewater treatment plants. Acs Sustain. Chem. Eng. 2 (7), 1656–1665.

Lv, X.Y., Gao, B., Sun, Y.Y., Shi, X.Q., Xu, H.X., Wu, J.C., 2014. Effects of humic acid and solution chemistry on the retention and transport of cerium dioxide nanoparticles in saturated porous media. Water Air Soil Pollut. 225 (10).

McKenzie, N., Jacquier, D., Isbell, R., Brown, K., 2004. Australian Soils and Landscapes. Csiro Publishing, Collingwood.

Mudunkotuwa, I.A., Grassian, V.H., 2010. Citric acid adsorption on TiO2 nanoparticles in aqueous suspensions at acidic and circumneutral pH: surface coverage, surface speciation, and its impact on nanoparticle-nanoparticle interactions. J. Am. Chem. Soc. 132 (42), 14986–14994.

Park, B., Donaldson, K., Duffin, R., Tran, L., Kelly, F., Mudway, I., Morin, J.P., Guest, R., Jenkinson, P., Samaras, Z., Giannouli, M., Kouridis, H., Martin, P., 2008. Hazard and risk assessment of a nanoparticulate cerium oxide-based diesel fuel additive – a case study. Inhal. Toxicol. 20 (6), 547–566.

Rhoades, J., 1982. In: Page, A. (Ed.), Methods of Soil Analysis: Part 2: Chemical and Microbiological Properties. ASA, Madison, WI.

Taha, M., Taha, O., 2012. Influence of nano-material on the expansive and shrinkage soil behavior. J. Nanoparticle Res. 14 (10), 1–13.

Torkzaban, S., Bradford, S.A., Vanderzalm, J.L., Patterson, B.M., Harris, B., Prommer, H., 2015. Colloid release and clogging in porous media: effects of

solution ionic strength and flow velocity. J. Contam. Hydrol. 181, 161–171.
VandeVoort, A.R., Skipper, H., Arai, Y., 2014. Macroscopic assessment of nanosilver toxicity to soil denitrification kinetics. J. Environ. Qual. 43 (4), 1424–1430.
Wang, Y.F., Westerhoff, P., Hristovski, K.D., 2012. Fate and biological effects of silver, titanium dioxide, and C-60 (fullerene) nanomaterials during simulated wastewater treatment processes. J. Hazard. Mater. 201, 16–22.
Wang, D., Ge, L., He, J., Zhang, W., Jaisi, D.P., Zhou, D., 2014. Hyperexponential and nonmonotonic retention of polyvinylpyrrolidone-coated silver nanoparticles in an Ultisol. J. Contam. Hydrol. 164, 35–48.
Weir, A., Westerhoff, P., Fabricius, L., Hristovski, K., von Goetz, N., 2012. Titanium dioxide nanoparticles in food and personal care products. Environ. Sci. Technol. 46 (4), 2242–2250.
Zhou, D., Keller, A.A., 2010a. Role of morphology in the aggregation kinetics of ZnO nanoparticles. Water Res. 44 (9), 2948–2956.
Zhou, D.X., Keller, A.A., 2010b. Role of morphology in the aggregation kinetics of ZnO nanoparticles. Water Res. 44 (9), 2948–2956.
Zhou, D.X., Abdel-Fattah, A.I., Keller, A.A., 2012. Clay particles destabilize engineered nanoparticles in aqueous environments. Environ. Sci. Technol. 46 (14), 7520–7526.
Zhou, D.X., Ji, Z.X., Jiang, X.M., Dunphy, D.R., Brinker, J., Keller, A.A., 2013. Influence of material properties on TiO2 nanoparticle agglomeration. PLoS One 8 (11).